THE BALTIC JOURNAL
OF ROAD
AND BRIDGE
ENGINEERING
2023/18(4)

ISSN 1822-427X/eISSN 1822-4288
2023 Volume 18 Issue 4: 145–165
https://doi.org/10.7250/bjrbe.2023-18.622

EXPERIMENTAL AND ANALYTICAL STUDIES OF STRING STEEL STRUCTURE FOR BRIDGES

EDMUNDAS BEIVYDAS[*1], ALGIRDAS JUOZAPAITIS[1], ILZE PAEGLITE[2]

[1]*Departament of Steel and Composite Structures, Faculty of Civil Engineering, Vilnius Tech, Vilnius, Lithuania*
[2]*Departament of Road and Bridge, Institute of Transport Infrastructure Engineering, Riga Technical University, Riga, Latvia*

Received 22 June 2023; accepted 15 November 2023

Abstract. Due to their efficiency, suspension structures are widely used in both roof slabs and different kinds of bridges, from which stress ribbon pedestrian bridges can be distinguished. The main disadvantage of the latter is high deformability, especially under asymmetrical loads. Recently, string structures or their systems have been introduced into bridge building. Numerical and experimental analysis of string behaviour under symmetrical and asymmetrical loads is carried out in the article. Analytical expressions for the calculation of string displacements and tensile forces are presented. The impact of the string pre-stress on the state of its stresses and deformations was evaluated. The assessment of the accuracy of analytical expressions by applying the results of numerical and experimental research is presented. A methodology is proposed for calculating the pre-stressing force taking into account the operational requirements. Three main loading options at different string pre-stress values are analysed. It is worth mentioning that the difference (error) between the analytical and numerical results is not extensive, it does not exceed 3%. It is necessary to notice that in all cases, the analytically obtained results are somewhat higher than FEM (numerically) obtained results.

* Corresponding author. E-mail: edmundas.beivydas@vilniustech.lt

Edmundas BEIVYDAS (ORCID ID 0009-0008-3318-0294)
Algirdas JUOZAPAITIS (ORCID ID 0000-0002-8067-6363)
Ilze PAEGLITE (ORCID ID 0000-0001-5810-2032)

Keywords: behaviour analysis, experimental study, numerical analysis, pre-stressed structure, string structure.

Introduction

Suspension structures, due to their excellent technical characteristics, are widely used in bridges of various types, including the pedestrian bridges (Gimsing & Georgakis, 2012; Ito, 2005; Parke & Hewson, 2022; Idelberger, 2011). Stress-ribbon bridges should be mentioned as the simplest structural solutions for that purpose (Strasky, 2011; Baus & Schlaich, 2008; Han et. al, 2016). With the lowest building (structure) height and, at the same time, the relatively small mass of the supporting structures, these bridges also have certain disadvantages. First of all, their curved outline due to the initial sag of the supporting element is not very well adapted to their operation. In addition, under the influence of traffic loads, especially the asymmetrical ones, these bridges experience large displacements (Caetano & Cunha, 2004; Radnić et al., 2015; Hu et al., 2013; Romera et al., 2020; Zhang et al., 2022). There are known reasons for these displacements and possible ways to stabilize the original shape of the bridge (Bleicher et al., 2011; Juozapaitis et al., 2006, 2021; Sandovič & Juozapaitis, 2012). In certain cases, this requires increasing not only the dead load (mass) of the bridge, but also the cross-section of the supporting suspended structure due to significantly increased tensile stresses (Markocki et al., 2013; Juozapaitis & Norkus, 2007; Susmitha et al., 2019).

One of the structural measures to improve the operational and behavioural characteristics of such bridges would be to apply straight suspension elements (see Figure 1) or their systems (Unitsky, 2006; Li et al., 2012, 2023; Beivydas, 2019, 2022a). Such supporting suspension elements without initial sag are also called strings. Most of the time, these structures are pre-stressed in order to meet the operational requirements (Li et al., 2015). They can be designed as separate supporting elements or can be used as an integral part of various combined constructions. In the past few decades, this type of constructions has been under analysis and used in the so-called string bridge systems or string rail structure, also called AERORail structures (Li et al., 2012, 2015, 2023). For the most part, numerical and experimental methods are used to analyse the behaviour of these structures (Li et al., 2012; Beivydas, 2020, 2022b). It should be noted that the analytical calculation methods of such string constructions,

especially those subjected to asymmetrical loads, are not sufficiently developed.

The article discusses the behaviour of a pre-stressed steel string under symmetrical and asymmetrical loads. The aim of the article is to analyse the behaviour of the string under symmetric and asymmetric loads and to present an analytical methodology for its calculation and to base this methodology on experimental research and numerical analysis. In the first section, the analytical calculation methodology of a fully flexible string is presented. The calculation methodology is presented separately, depending on the pre-tension of the string and the loading location of the structure (symmetrical and asymmetric load). A total of four different calculation options are provided.

The second section presents the numerical analysis of the string using the FEM method, under the same loads and pre-stress as in the analytical calculation. The results are compared with those obtained analytically and the obtained conclusions and observations are presented. In the second section, the structure is analysed using numerical and experimental methods. During both numerical and experimental research, analogous parameters and variants are analysed, as in the case of analytical calculation. This section discusses in more detail what parameters to use when modelling a structure numerically. A description of how the experimental study was conducted is also provided. In order to verify the accuracy of the analytical method, the results obtained by this method are compared with the results obtained by numerical and experimental methods. The results are presented both in the form of tables and graphs.

The last section presents the conclusions of the study. There are four main conclusions based on string pre-tension, loading variant (symmetrical and asymmetrical) and the results of all three methods (analytical, numerical, and experimental).

1. Displacements and forces of an elastic string

The analytical calculation methodology of the spring is developed taking into account the most dangerous loading cases for displacements and axial forces, i. e., when the live loads are placed over the whole string span and over half its span. It should be noted that this methodology can be applied to other loading cases (when the live load is distributed over the middle part of the span), but then additional solutions are necessary for the moment under such loads and to calculate the string length after deformation.

1.1. Non-prestressed flexible string. Symmetrical loading

As mentioned above, a flexible and elastic string can be pre-stressed or non-prestressed. An untensioned string is a suspended element whose initial length is equal to the length of the span ($s_0 = l$). Forces and displacements due to applied loads are assumed to occur without pre-stressing, i.e., the string does not receive any additional tensile force – pre-tension ($N_0 = 0$). N_0 – *string pretension force.*

The diagram of a non-stressed string symmetrically loaded with dead g and live v (traffic) loads is presented in Figure 1.

The equilibrium condition of such a flexible structure with respect to the middle of the span can be formulated as follows:

$$H = \frac{M(x)}{\Delta f}, \tag{1}$$

where:

$$M(x) = \frac{(g+v)l^2}{8}\left(\frac{4x}{l} + \frac{4x^2}{l^2}\right), \tag{1a}$$

$M(x)$ – the moment caused by external symmetric loads g (dead load) and v (live load) acting on the string, calculated at any point on the string;
H – tension force of the string;
Δf – elastic displacement of the string at mid-span;
g – dead load;
v – live (traffic) load;
l – span length;
x – horizontal axis coordinate.

Equation (1) shows that we have two interconnected unknown variables (H and Δf) and to determine them (as for all suspended structures) it is not sufficient to do that by static equilibrium equations

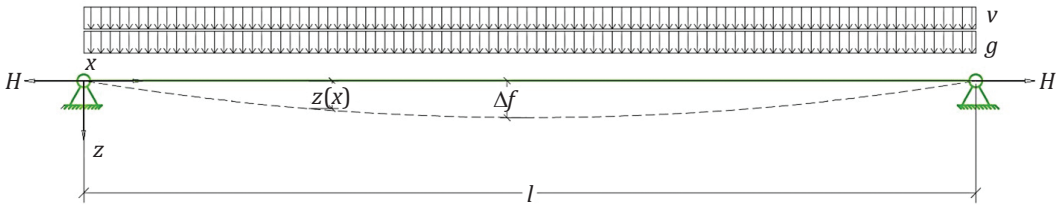

Figure 1. Diagram of a symmetrically loaded non-stressed string. Here v is live (traffic) load, g – dead load

alone. It is necessary to use, as usual, the deformations compatibility equation (2):

$$\Delta s_{\text{el}} = \Delta s_{\text{g}}, \tag{2}$$

where:

$\Delta s_{\text{el}} = Hl / EA$ – elastic elongation of the string;
$\Delta s_{\text{g}} = (s_1 - s_0)$ – geometric elongation of the string;
s_1 – post-deformation string length;
s_0 – pre-deformation string length;
E – elasticity modulus of the string;
A – string cross-section area.

Considering Equation (1), the curve of the deformed axis of a symmetrically loaded string can be obtained:

$$z(x) = \Delta f \left(\frac{4x}{l} + \frac{4x^2}{l^2} \right). \tag{3}$$

It is obviously a quadratic parabola.

Then the length of the string after deformation will be equal to:

$$s_1 = l + \frac{8}{3} \frac{\Delta f^2}{l}. \tag{4}$$

By using Equations (1), (2) and (4), we will get a known solution for calculating the displacement of a symmetrically loaded string in the middle of the span:

$$\Delta f = \sqrt[3]{\frac{3(g+v)l^4}{64EA}}. \tag{5}$$

Analogously, from Equations (1), (2) and (4) we get a direct solution for calculating the tensile force:

$$H = \sqrt[3]{\frac{(g+v)^2 l^2 EA}{24}}. \tag{6}$$

The expression in Equation (6) is identical to the one presented (Schlaich et al., 2011). Equations (5) and (6) show that it is possible to calculate the displacement of a non-stressed string in the middle of the span and its tension force without iterations, if the string loads, span length and its axial stiffness are known. If the elastic displacement of the string is known Δf, it is possible to calculate the tensile force using Equation (1). It is clear that the tension force of the string depends on the values of the displacement and will be significantly higher than that of the cable of similar parameters, which has an initial sag (Kulbach, 2007; Schlaich et al., 2011).

1.2. Non-prestressed flexible string. Asymmetrical loading

It is known that in an asymmetrically loaded cable, there are also displacements of kinematic origin, which often exceed elastic displacements (Gimsing & Georgakis, 2012. Juozapaitis & Norkus, 2007).

Elastic string asymmetrically loaded with live (traffic) load and symmetrically dead load (Figure 2) should be analysed.

It is necessary to note that the flexible string as a suspension element is formed without an initial sag ($f_0 = 0$) and, therefore, compared to a cable, does not have kinematic displacements under the action of an asymmetric load. Only elastic displacements will act on the string loaded in this way, and the curve of its deformed axis is described by the sum of two elastic displacement curves (similar to acting moments):

$$z_l(x) = \frac{\Delta f_{as}}{1+0{,}5\gamma}\left[\left(\frac{4x}{l}-\frac{4x^2}{l^2}\right)+\frac{\gamma}{2}\left(\frac{6x}{l}-\frac{6x^2}{l^2}\right)\right], \quad (7)$$

where $0 \le x \le \frac{l}{2}$,

$$z_r(x) = \frac{\Delta f_{as}}{1+0{,}5\gamma}\left[\left(\frac{4x}{l}-\frac{4x^2}{l^2}\right)+\frac{\gamma}{2}\left(\frac{2x}{l}-2\right)\right], \quad (8)$$

where $\frac{l}{2} \le x \le l$;
where:

$z_l(x)$ – displacements of the asymmetrically loaded (left) part;

$z_r(x)$ – displacements of the (right) part loaded only with symmetrical load;

$\gamma = v / g$ – ratio of live and dead loads;

Δf_{as} – displacement of an asymmetrically loaded string at mid-span.

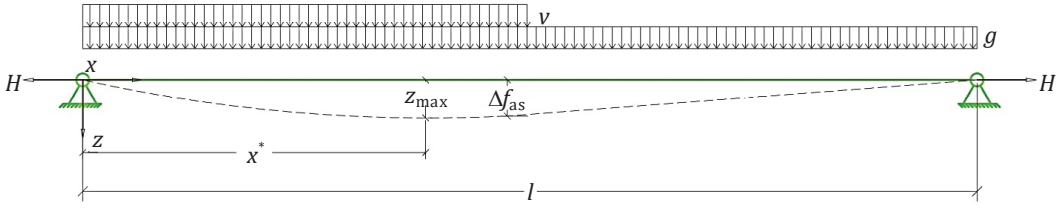

Figure 2. Design scheme of an asymmetrically loaded non-stressed string where: z_{max} – maximum displacements of the asymmetrically loaded (left) part, Δf_{as} – displacement of an asymmetrically loaded string at mid-span, x^* – the horizontal distance from the origin of the coordinates to the point of maximum displacement, v – live (traffic) load, g – dead load, H – shear force, l – span length

Equations (7) and (8) show that the curve of the deformed axis of the left asymmetrically loaded part is the sum of two quadratic parabolas, and the right one is the sum of a quadratic parabola and a straight line.

As in the case of symmetrical loading, one can use static equilibrium equations to obtain an expression for calculating the tensile force:

$$H_{\text{as}} = \frac{M_{\text{as}}(x)}{\Delta f_{\text{as}}} = \frac{\frac{gl^2}{8} + \frac{vl^2}{16}}{\Delta f_{\text{as}}} = \frac{gl^2}{8\Delta f_{\text{as}}}\left(1 + \frac{\gamma}{2}\right). \tag{9}$$

The total length of an asymmetrically loaded string after deformation is calculated using the sum of the geometric lengths of its individual parts:

$$s_{\text{as}} = s_{\text{l}} + s_{\text{r}} = l + \frac{8\Delta f_{\text{as}}^2}{3l^2} \cdot \frac{\left(1 + \gamma + \frac{5\gamma^2}{16}\right)}{\left(1 + \gamma + \frac{\gamma^2}{4}\right)}, \tag{10}$$

or

$$s_{\text{as}} = l + \frac{8\Delta \text{f}_{\text{as}}^2}{3l^2} \cdot \Psi, \tag{10a}$$

where: $\Psi = \left(1 + \gamma + \frac{5\gamma^2}{16}\right) / \left(1 + \gamma + \frac{\gamma^2}{4}\right)$.

Then the displacement of the asymmetrically loaded string at the mid-span and its tensile force are calculated as follows:

$$\Delta f_{\text{as}} = \sqrt[3]{\frac{3g(1 + 0{,}5\gamma)l^4}{64EA\Psi}}; \tag{11}$$

$$H_{as} = \sqrt[3]{\frac{g^2 l^2 EA(1 + 0{,}5\gamma)^2 \Psi}{24}}. \tag{12}$$

Equations (11)–(12) are analogous to Equations (5)–(6), the only difference is that they additionally evaluate the γ influence of the ratio of asymmetric and symmetric loads on displacements and tensile forces. Under identical initial conditions, the displacement and tensile force values of an asymmetrically loaded string will be smaller than those of a symmetrically loaded string.

1.3. Pre-stressed string. Symmetrical loading

The elastic string can be pre-stressed in order to reduce its displacements. The values of the pre-stressing force are selected according to operational requirements and applied loads. It is assumed that the string can be pre-stressed before the dead load is applied.

Displacements of such a pre-stressed string in the middle of the span are calculated analogously to a non-stressed string by applying Equations (1)–(4). However, in this case the elastic elongation is calculated, where N_0 is the pre-stressing force. An expression can then be obtained to calculate the displacement of the pre-stressed string:

$$\Delta f_{\text{pr}} = \sqrt[3]{\frac{3pl^4\left(1-n\right)}{64EA}}, \tag{13}$$

where:

$$n = \frac{N_0}{H_{pr}}, \tag{14}$$

n – a ratio of pre-stressing force to tensile force;
N_0 – pre-stressing force;
H_{pr} – tension force after applying the load.

Analogously, the formula for calculating the tensile force of a pre-stressed string can be obtained:

$$H_{\text{pr}} = \sqrt[3]{\frac{p^2l^2EA}{24\left(1-n\right)}}. \tag{15}$$

It is important to note that Equations (13) and (15) are analogous to the formulas of a non-stressed string for calculating displacement and tension force. The analysis of Equations (13), (15) proves that pre-stressing reduces the elastic displacement of the string; however, at the same time it increases the tensile force. It is necessary to note that the values of the ratio should be selected according to the operational requirements.

1.4. Pre-stressed string. Asymmetrical loading

In case of asymmetrical load of the pre-stressed string, taking into consideration Equations (7)–(10), its displacement in the middle of the span will be equal to:

$$\Delta f_{\text{as,pr}} = \sqrt[3]{\frac{3g\left(1+0.5\gamma\right)l^4\left(1-n\right)}{64EA\Psi}}. \tag{16}$$

Analogously, the formula for calculating the tensile force of such a string can be obtained:

$$H_{\text{as,pr}} = \sqrt[3]{\frac{g^2l^2EA\left(1+0.5\gamma\right)^2\Psi}{24\left(1-n\right)}}. \tag{17}$$

Equations (16)–(17) prove that, just like in the case of symmetrical load, pre-stressing reduces string displacements but increases the tensile force.

2. Numerical analysis and experimental investigation of elastic string

In order to determine the accuracy of analytically obtained calculation formulas, a numerical analysis of the elastic string under symmetrical and asymmetrical loads was performed. The finite element program Autodesk Robot Structural Analysis was used for the calculations. The string was modelled as a flexible pre-stressed cable element. The supports were modelled as fixed for linear inclinations, but movable for angular displacements. The geometrical parameters of the string were selected according to the dimensions of the experimental model:

- string span L – 5.0 m;
- the string cross-section of a steel round bar with a diameter of 6 mm, steel class S420;
- during the test, the elastic modulus E of the steel of the string was determined to be 202.8 GPa.

In Autodesk Robot Structural Analysis, pre-stressing can be specified as a separate parameter. Two options were modelled (according to the data obtained in the experiment), when the pretension of the string N_0 was equal to 5.25 kN and 6.625 kN. In order to make the calculations as accurate as possible, the 5-meter string was divided into 60 separate finite elements in the model. When designing and calculating a cable element, Autodesk Robot performed calculations non-linearly. Geometric nonlinearity was calculated by evaluating *large displacements.*

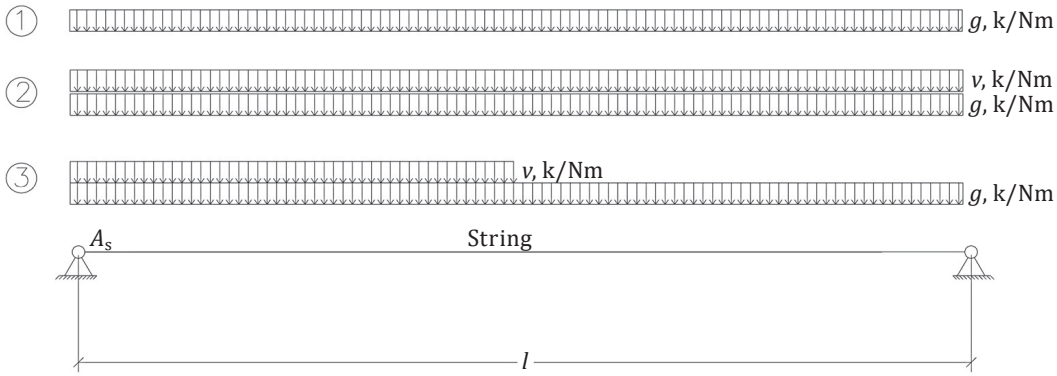

Figure 3. String loading scheme: 1 – dead loading; 2 – symmetrical live loading; 3 – asymmetrical live loading. Here: v – live (traffic) load, g – dead load, L – span length

Three main loading options at different string pre-stress values were analysed. The results of the analysis are presented in Tables 1 and 2. It is worth mentioning that the difference (error) between the analytical and numerical results is not extensive, it does not exceed 3%. It should be noted that in all cases, the analytically obtained results are somewhat higher than FEM (numerically) obtained results. In Figure 3, the string loading diagram is presented, and the numerical values of the loads can be seen in Tables 1–4.

The attained results of stresses and tensile forces are presented in Tables 1 and 2, and those of displacements – in Tables 3 and 4, taking into account the pre-stress forces of the string and the load variants. In total, the string was loaded in five different ways: two times symmetrical load (dead and live loads) were applied and three times – asymmetrical load.

The tables show the stresses and forces when the pre-stressing force in the string N_0 was equal to 5.25 kN and 6.625 kN. The left columns of the tables present the load variants, the right columns show the

Table 1. Stresses and tensile forces under the pre-stressing force of the string N_0 = 5.25 kN

Load option	Loads		Analytical results		Numerical results		Difference, %
	Dead load, kN/m	Live load, kN/m	Stresses, MPa	Axial force, kN	Stresses, MPa	Tensile force, kN	
Dead load, No. 1	0.17		246.56	6.97	247.35	7.00	0,3%
Live load, Symmetrical	0.17	0.17	366.45	10.36	361.31	10.23	–1.4%
Live load, Asymmetrical γ=1	0.17	0.17	312.67	8.84	308.42	8.73	–1.4%
Live load, Asymmetrical γ=2	0.17	0.34	373.00	10.54	365.91	10.36	–1,9%
Live load, Asymmetrical γ=3	0.17	0.51	428.61	12.11	419.80	11.88	–2.1%

Table 2. Stresses and tensile forces under the pre-stressing force of the string N_0 = 6.625 kN

Load option	Loads		Analytical results		Numerical results		Difference, %
	Dead load, kN/m	Live load, kN/m	Stresses, MPa	Axial force, kN	Stresses, MPa	Tensile force, kN	
Dead load	0.17		256.57	7.25	257.00	7.26	0,2%
Live load, Symmetrical	0.17	0.17	377.97	10.68	369.34	10.45	–2.3%
Live load, Asymmetrical γ=1	0.17	0.17	323.62	9.15	316.88	8.97	–2.1%
Live load, Asymmetrical γ=2	0.17	0.34	384.59	10.87	373.91	10.58	–2.9%
Live load, Asymmetrical γ=3	0.17	0.51	440.67	12.45	427.52	12.10	–3.1%

Table 3. Vertical displacements of the string in the middle of the span when N_0=5.25 kN

Load type	Loads		Analytical results	Numerical results	Difference, %
	Dead load, kN/m	Live load, kN/m	Vertical displacements, mm		
Dead load, No. 1	0.17		–76.2	–76.5	0.4%
Live load, Symmetrical	0.17	0.17	–102.6	–104.5	1.8%
Live load, Asymmetrical γ=1	0.17	0.17	–90.2	–91.5	1.4%
Live load, Asymmetrical γ=2	0.17	0.34	–100.8	–102.6	1.8%
Live load, Asymmetrical γ=3	0.17	0.51	–109.7	–111.7	1.8%

Table 4. Vertical displacements of the string in the middle of the span when N_0 = 6.625 kN

Load type	Loads		Analytical results	Numerical results	Difference, %
	Dead load, kN/m	Live load, kN/m	Vertical displacements, mm		
Dead load	0.17		–73.3	–73.5	0.3%
Live load, Symmetrical	0.17	0.17	–99.5	–102.1	2.5%
Live load, Asymmetrical γ=1	0.17	0.17	–87.1	–88.9	2.0%
Live load, Asymmetrical γ=2	0.17	0.34	–97.8	–100.2	2.4%
Live load, Asymmetrical γ=3	0.17	0.51	–106.7	–109.5	2.6%

a) Symmetrical loading, where N_0=6.625 kN

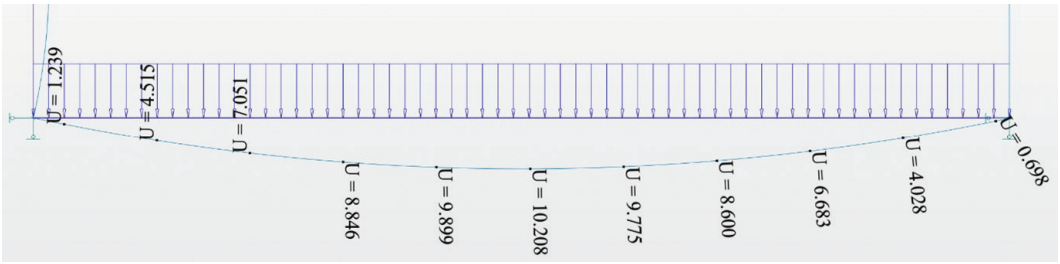

b) asymmetrical loading, where N_0=6.625 kN, γ=2

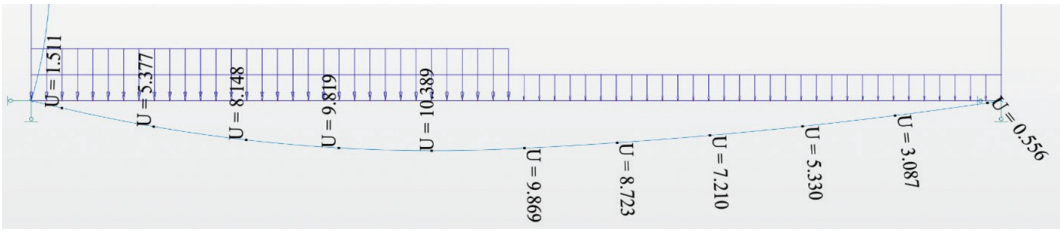

Figure 4. Displacements from Autodesk Robot Structural Analysis

numerical and analytical results, and the ratio differences between the numerical and analytical results are expressed as percentage.

The pre-stress forces and loads of the strings were selected based on the data obtained and measured during the experiment and also by applying the loads used during the experiment.

Graphs of string displacements under symmetric and asymmetric loading are presented in Figure 4. These graphs show that the displacements of an asymmetrically loaded string (when $\gamma = 2$) are approximately 1.8% higher than in the case of symmetrical loading. It should be noted that the maximum displacement of an asymmetrically loaded string is not far from the string mid-span. The coordinate of the maximum displacement can be determined from the analytical expressions, see Equation (7). This expression shows that the higher the value of the load ratio γ, the more the location (coordinate) of the maximum displacement moves away from the middle of the span. In addition, it is possible to determine at what value the displacements of an asymmetrically loaded string become larger than the displacements of a symmetrically loaded string.

To sum up the results of the analysis, it can be stated that the differences between numerical and analytical calculations do not exceed 3%. Therefore, a statement can be made that the obtained analytical string calculation formulas are sufficiently accurate.

2.1. Experimental program

As mentioned in the previous section, in order to study the behaviour of the string, an experimental study of the string model was also carried out. The string model parameters were as follows:

- string span $L = 5.0$ m;
- the string cross-section of a steel round bar with a diameter of 6 mm, steel class S420;
- during the test, the elastic modulus E of the steel of the string was determined to be 202.8 GPa.

The model structure was loaded with a uniformly distributed load using weights made from rectangular steel bars with dimensions of 25 mm × 25 mm, length of 500 mm, where the calculated mass of one weight was 2.45 kg.

Digital gauge was used to measure displacements: Novotechnik TYP:TR-0100, ART No 023264, F.NR 119988/A. The vertical displacements of the model were measured at 13 points, excluding the measurement of the horizontal displacements of the supports. The tension of the string was measured by stress gauges – resistance sensors with a base of 20 mm (and a resistance of $R = 202.3\ \Omega$), at the point marked with the number 14 – u, the layout of which is shown in Figure 5. All sensors were connected to the device Ahlborn almemo 5990-2, which was used to obtain all the data.

Figures 7–12 and Tables 5–6 present the results of experimental and numerical analysis. The graphs and tables show the stresses and displacements of one of the strings, since the displacements were measured jointly for both strings. The stresses were measured separately in both strings, but the absolute difference in the stresses was only 4%, and the change in stresses, depending on the loading option, varied by up to 1.5% in different strings. This is the reason why the comparison of the results includes the measurement of the stresses and tensile forces of only one of the string results.

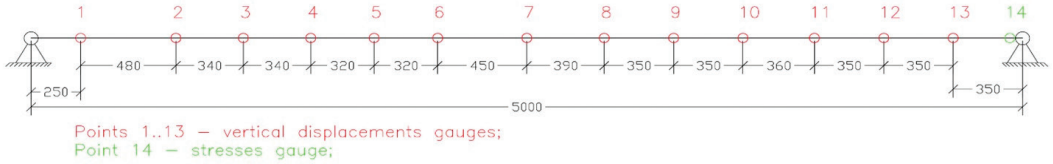

Figure 5. Diagram of vertical displacements and stress gauges

Figure 6. Photo of experimental model

Table 5. Numeric and experimental results, where pre-stressing force of the string N_0 = 5.25 kN

Load option	Loads		Experimental results		Numerical results		Difference, %
	Dead load, kN/m	Live load, kN/m	Stresses, MPa	Axial force, kN	Stresses, MPa	Axial force, kN	
Dead load	0.17		247.35	6.99	247.35	7.00	0%
Live load, Symmetrical	0.17	0.17	358.30	10.13	361.31	10.23	1%
Live load, Asymmetrical γ=1	0.17	0.17	308.29	8.71	308.42	8.73	0%
Live load, Asymmetrical γ=2	0.17	0.34	363.74	10.28	365.91	10.36	1%
Live load, Asymmetrical γ=3	0.17	0.51	413.90	11.70	419.80	11.88	1%

Table 6. Numeric and experimental results, where pre-stressing force of the string N_0 = 6.625 kN

Load option	Loads		Experimental results		Numerical results		Difference, %
	Dead load, kN/m	Live load, kN/m	Stresses, MPa	Axial force, kN	Stresses, MPa	Axial force, kN	
Dead load	0.17		257.00	7.26	257.00	7.26	0%
Live load, Symmetrical	0.17	0.17	354.50	10.02	369.34	10.45	4%
Live load, Asymmetrical γ=1	0.17	0.17	313.34	8.86	316.88	8.97	1%
Live load, Asymmetrical γ=2	0.17	0.34	364.61	10.30	373.91	10.58	2%
Live load, Asymmetrical γ=3	0.17	0.51	412.91	11.67	427.52	12.10	3%

The obtained results reveal the accuracy of the analytical and numerical results, since the experimentally obtained and measured stresses differ by up to 4%.

In order to compare the results obtained numerically and analytically, Figures 7–12 present graphs of the vertical displacements in each measured section (see Figure 5). Markings in graphs: No. 1, when pre-stressing force N_0 = 5.25 kN; No. 2, when pre-stressing force N_0 = 6.625 kN.

Figures 7–10 show that the differences between the experimental and numerical results are minimal. The biggest differences in extremes are up to 3%. Since the numerical results have already been compared with the analytical ones, and differences of a similar value have been obtained, it can be stated that the presented analytical methodology is accurate.

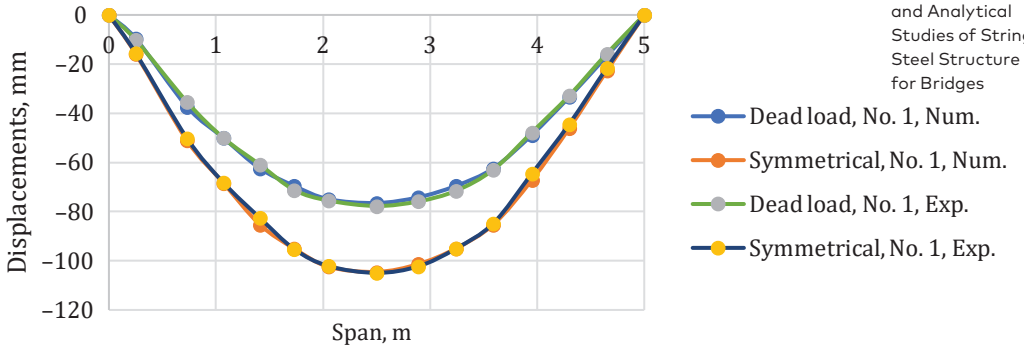

Figure 7. Numerical and experimental results of vertical displacements, where: No. 1 – test number 1 with string pre-tension N_0 = 5.25 kN, Num – a numerical calculation method, Exp – an experimental method, symmetrical – the live load is symmetrical over the entire length of the span

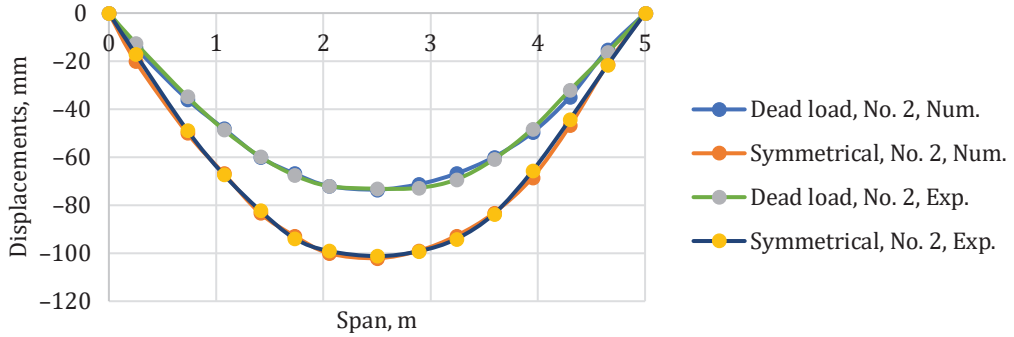

Figure 8. Numerical and experimental results of vertical displacements where: No. 2 – test number 2 with string pre-tension N_0 = 6.625 kN, Num – a numerical calculation method, Exp – an experimental method, symmetrical – the live load is symmetrical over the entire length of the span

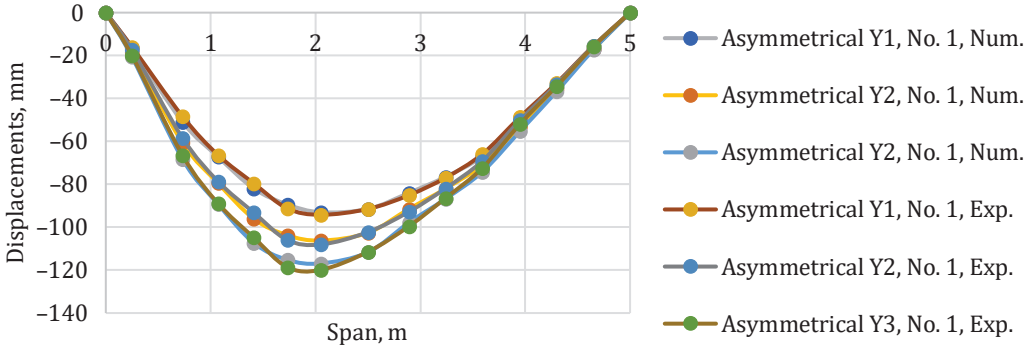

Figure 9. Numerical and experimental results of vertical displacements where: No. 1 – test number 1 with string pre-tension N_0 = 5.25 kN, Num – a numerical calculation method, Exp – an experimental method, asymmetrical – live load asymmetrical. The left side of the string is loaded, $\gamma = v/g$ – a ratio of live and dead loads

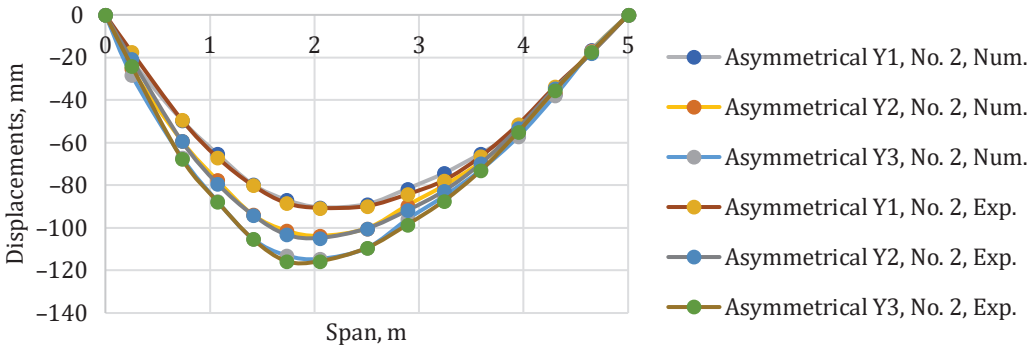

Figure 10. Numerical and experimental results of vertical displacements where: No. 2 – test number 2 with string pre-tension N_0 = 6.625 kN, Num – a numerical calculation method, Exp – an experimental method, asymmetrical – live load asymmetrical. The left side of the string is loaded, $\gamma = v/g$ – a ratio of live and dead loads

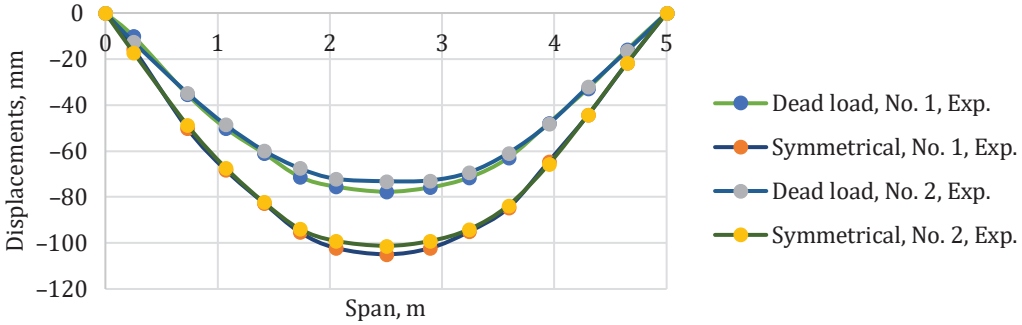

Figure 11. Experimental results of vertical displacements where: No. 1 – test number 1 with string pre-tension N_0 = 5.25 kN, No. 2 – test number 2 with string pre-tension N_0 = 6.625 kN, Exp – an experimental method, symmetrical – the live load is symmetrical over the entire length of the span

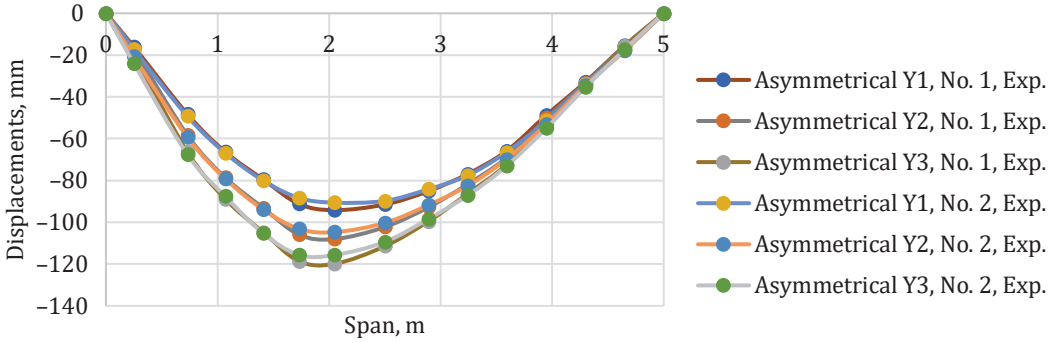

Figure 12. Experimental results of vertical displacements where: No. 1 – test number 1 with string pre-tension N_0 = 5.25 kN, No. 2 – test number 2 with string pre-tension N_0 = 6.625 kN, Exp – an experimental method, asymmetrical – live load asymmetrical. The left side of the string is loaded, $\gamma = v/g$ – a ratio of live and dead loads

Figures 11–12 present the graphs of experimental model results only. The results are presented for two different values of pre-stressing force N_0 = 5.25 and 6.625 kN. The graphs show that the pre-stress reduces the maximum displacements of the string. After increasing the string pre-stressing force N_0 from 5.25 kN to 6.625 kN, string displacements, both in the case of symmetrical loading and in the case of asymmetrical loads, decreased by 3.6%.

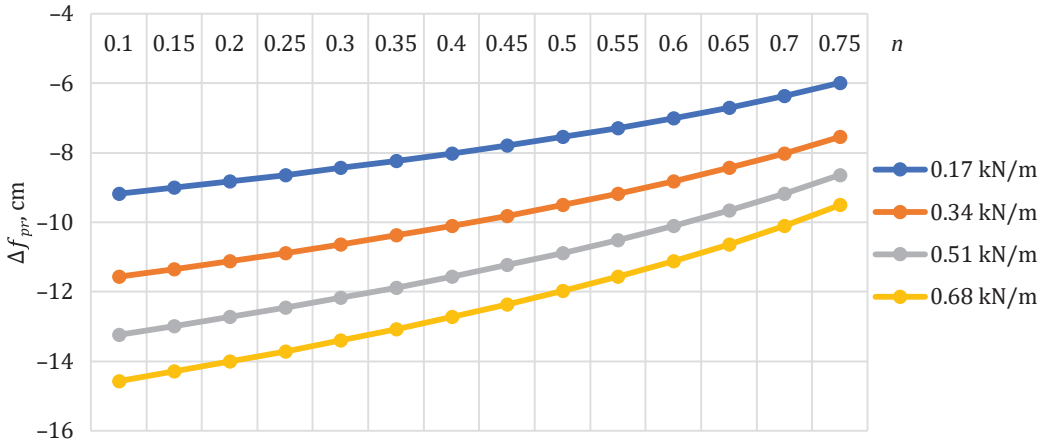

Figure 13. Dependence of vertical displacements on the string pre-stressing parameter *n*, when the string is loaded symmetrically. The specified load values in the legend are the total sum of live and dead load

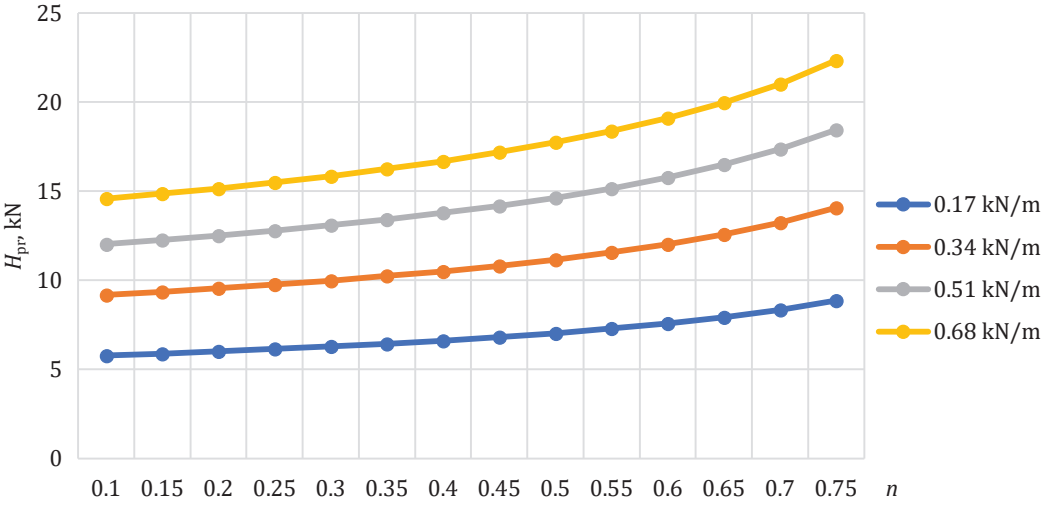

Figure 14. Dependence of tensile force in the string on the string pre-stressing parameter *n*, when the string is loaded symmetrically. The specified load values in the legend are the total sum of live and dead load

In order to more accurately show the impact of the string pre-stress on its displacements, Figure 13 presents the following graph – the dependence of the displacements of the string on the pre-stressing parameter *n*, value from 0.1 to 0.75 (according to the geometry of the experimental model), see Equation (13). Figure 14 shows the dependence of the tension force on the same parameter *n*.

Figure 13 and Figure 14 clearly show the impact of string pre-stress. The higher the string pre-stress value, the smaller the string displacement. Reducing the displacement of the string and increasing the pre-stress in the string will definitely cause the tension force to increase as well.

Conclusions

The article has discussed the behaviour of the stressed and pre-stressed steel strings under symmetrical and asymmetrical loads. Analytical expressions have been presented for the calculation of the displacements and tension forces of such a suspension structure while taking into account the applied loads and the initial string pre-stress. Moreover, the numerical and physical experiments of such string model have been performed. Based on the obtained results, the following conclusions can be drawn:

1. The original formulas for the direct calculation of displacements and tension forces of the asymmetrically loaded pre-stressed and non-stressed flexible string have been obtained. It has been established that only elastic deformations will act on the string loaded asymmetrically while displacements of kinematic origin do not happen since it does not have the initial sag ($f_0 = 0$). It has been found that under identical initial conditions the displacement and tensile force values of an asymmetrically loaded string will be smaller than those of a symmetrically loaded string.
2. The effect of the string pre-stress force for the string stress-strain state has been evaluated. It has been established that by increasing the string pre-stress value N_0 (or ratio), it is possible to reduce its displacements by the required amount both under symmetrical and under asymmetrical loads. Displacements of such a pre-stressed string are calculated analogously to a non-stressed string. Moreover, it has been observed that a pre-stress value simultaneously increases the tensile force of the string.
3. The impact of the asymmetrical load on the string displacements and strains has also been taken into account. It has been discovered that by increasing the values of the load ratio ɣ from 1 to 3, the maximum

string displacement goes by 22.1%. In addition, as the value of ɣ increases, the location of the maximum displacement shifts from the middle of the span to the side of the asymmetric load. However, even with high gamma values, it does not reach span quarter, as it is typical of cables.

4. The spot-on accuracy of analytical expressions for calculating displacements and strains of a flexible string has been confirmed by both numerical and physical experiments. The most considerable errors (in comparison with the numerical analysis) have not exceeded 3–4%.

REFERENCES

Baus, U., & Schlaich, M. (2008). *Footbridges. Construction, Design, History*. Birkhäuser, Basel. https://doi.org/10.1007/978-3-7643-8222-3

Beivydas, E. (2019). A simplified calculation method for symmetrical loading of a single-span composite string steel structure. *Engineering Structures and Technologies*, *11*(2), 70–73. https://doi.org/10.3846/est.2019.11323

Beivydas, E. (2022a). Parametrical analysis for symmetrical loading of a single-span composite string steel structure. *The Eurasia Proceedings of Science, Technology, Engineering & Mathematics*, *17*, 90–101. https://doi.org/10.55549/epstem.1176065

Beivydas, E. (2022b). Analysis for symmetrical and asymmetrical loading of a single-span combined string steel structure. *Engineering Structures and Technologies*, *14*(1), 1–6. https://doi.org/10.3846/est.2022.18403

Beivydas, E. (2020). Suspension string future structure. *ABSE Symposium, Wroclaw 2020: Synergy of Culture and Civil Engineering – History and Challenges, Report* (pp. 733–740). https://doi.org/10.2749/wroclaw.2020.0733

Bleicher, A., Schlaich, M., Fujino, Y., & Schauer, T. (2011). Model-based design and experimental validation of active vibration control for a stress ribbon bridge using pneumatic muscle actuators. *Engineering Structures*, *33*, 2237–2247. https://doi.org/10.1016/j.engstruct.2011.02.035

Caetano, E., & Cunha, A. (2004). Experimental and numerical assessment of the dynamic behaviour of a stress-ribbon footbridge. *Journal of Structural Concrete*, *5*(1), 29–38. https://doi.org/10.1680/stco.2004.5.1.29

Gimsing, N. J., & Georgakis, Ch. T. (2012). *Cable supported bridges: Concept and design* (3rd ed.). John Wiley & Sons. https://doi.org/10.1002/9781119978237

Han, K.-J., Lim, N.-H., Ko, M.-G., & Kim, K.-D. (2016). Efficient assumption of design variables for stress ribbon footbridges. *KSCE Journal of Civil Engineering*, *20*(1), 250–260. https://doi.org/10.1007/s12205-015-0186-6

Hu, W.-H., Caetano, E., & Cunha, A. (2013). Structural health monitoring of a stress-ribbon footbridge. *Engineering Structures*, *57*, 578–593. https://doi.org/10.1016/j.engstruct.2012.06.051

Idelberger, K. (2011). *The world of footbridges*. Ernst and Sohn GmbH. https://doi.org/10.1002/9783433600849

Ito, M. (2005). Cable-supported bridges. In W.F. Chen, & E.M. Lui (Eds.), *Handbook of Structural Engineering*. CRC Press.

Juozapaitis, A., & Norkus, A. (2007). Determination of rational parameters for the advanced structure of a pedestrian suspension steel bridge. *Baltic Journal of Road and Bridge Engineering*, *2*(4), 173–181. https://bjrbe-journals.rtu.lv/article/view/1822-427X.2007.4.173%E2%80%93181

Juozapaitis, A., Vainiunas, P., & Kaklauskas, G. (2006). A new steel structural system of a suspension pedestrian bridge. *Journal of Constructional Steel Research*, *62*(12), 1257–1263. https://doi.org/10.1016/j.jcsr.2006.04.023

Juozapaitis, A., Sandovič, G., Jakubovskis, R., & Gribniak, V. (2021). Effects of flexural stiffness on deformation behaviour of steel and FRP stress-ribbon bridges. *Applied Sciences*, *11*(6), Article 2585. https://doi.org/10.3390/app11062585

Kulbach, V. (2007). *Cable structures. Design and static analysis*. Estonian Academy Publishers.

Li, F., Guo, Z., Cui, Y., & Wu, P. (2023). Dynamic load test and contact force analysis of the AERORail structure. *Applied Sciences*, *13*(3), Article 2011. https://doi.org/10.3390/app13032011

Li, F., & Wu, P. (2015). Dynamic behaviors of pretensioned cable AERORail structure. *Journal of Central South University*, *22*, 2267–2276. https://doi.org/10.1007/s11771-015-2751-z

Li, F., Wu, P., & Liu, D. (2012). Experimental study on the cable rigidness and static behaviors of AERORail structure. *Steel and Composite Structures*, *12*(5), 427–444. https://doi.org/10.12989/scs.2012.12.5.427

Markocki, B., Makar, S., & Rogowski, R. (2013). Wybrane problemy w realizacji konstrukcji wstęgowej z betonu sprężonego na podstawie kładki pieszo-jezdnej w miejscowości Lubień. *Konstrukcje – Elementy – Materiały. Przegląd Budowlany*, *1*, 40–45. https://yadda.icm.edu.pl/baztech/element/bwmeta1.element.baztech-article-BTB6-0007-0099

Parke, G., & Hewson, N. (2022). *ICE Manual of Bridge Engineering* (3rd ed.). ICE publishing.

Radnić, J., Matešan, D., & Buklijaš-Kobojević, D. (2015). Numerical model for analysis of stress-ribbon bridges. *Građevinar*, *67*(10), 959–973. https://doi.org/10.14256/JCE.1383.2015

Romera, L., Hernández, S., Baldomir, A., & Nieto, F. (2020). Study of pedestrian comfort in a three span stress ribbon footbridge with carbon fibre cables. *WIT Transactions on The Built Environment, 196*(14), 139–152. https://doi.org/10.2495/HPSM200151

Sandovič, G., & Juozapaitis, A. (2012). The analysis of the behaviour of an innovative pedestrian steel bridge. *Procedia Engineering Steel Structures and Bridges 2012, 23rd Czech and Slovak International Conference, 40*. Elsevier Science Ltd. https://doi.org/10.1016/j.proeng.2012.07.117

Schlaich, M., Bogle, A., & Bleicher, A. (2011). *Entwerfen und Konstruieren Massivbau*. Institut für Bauingenieurwesen Technische universitat Berlin.

Strasky, J. (2011). *Stress ribbon and cable-supported pedestrian bridges* (2nd ed.). ICE Publishing. https://doi.org/10.1680/srcspb.41462

Susmitha, B., Vimala Priya, T., Veera Butchi Babu, J., Venkata Akhil, R., & Rajesh, V. (2019). Stress ribbon bridge analysis and design. *Journal of Emerging Technologies and Innovative Research*, *6*(3), 638–644. https://www.jetir.org/papers/JETIR1903584.pdf

Unitsky, A. (2006). *String transport in questions and answers*. STU Ltd. https://unitsky.engineer/assets/files/shares/2006/2006_26.pdf

Zhang, Yi., Pu, W., Zhang, Q., Liu, K., & Dong, H. (2022). Effect of ground motion orientation on seismic responses of an asymmetric stress ribbon pedestrian bridge. *Advances in Civil Engineering*, *2022*, Article e1278314. https://doi.org/10.1155/2022/1278314